CO_2 separation with carbon membranes in high pressure and elevated temperature applications

[a]Shamim Haider, [a]Arne Lindbråthen, [a]Jon Arvid Lie, [b]Ingerid Caroline Tvenning Andersen, [a]May-Britt Hägg*

[a]Norwegian University of Science and Technology, NTNU, Department of Chemical Engineering, 7491 Trondheim, Norway

[b]Metrohm Nordic AS, 1363 Høvik, Norway

***Corresponding author: Tel: +47 93080834. Email: may-britt.hagg@ntnu.no**

Highlights:

Carbon membranes testing at high pressure and elevated temperature

Single stage separation system for CO_2/CH_4 separation

Pore tailoring of carbon hollow fibers

Pilot scale-module construction of carbon hollow fibers

Abstract

Carbon hollow fibers (CHF) were fabricated by carbonization of deacetylated cellulose acetate precursor. To enhance membrane permeation properties, pore structure was tailored by means of an oxidation and reduction process followed by chemical vapor deposition with propene. Permeation properties using shell-side feed configuration of 70 modules (0.2-2 m^2) for both CHF and modified carbon hollow fibers (MCHF) were investigated for single gases, N_2 and CO_2 at high pressure (2-70 bar feed vs 0.05-1bar permeate pressure) and temperature from 25-120 °C. Maximum CO_2 permeance value for a MCHF module was recorded 50,000 times higher as compared to prior modification, and CO_2/N_2 selectivity was improved 41 times in comparison with CHF for the same module. Results indicated that carbon membranes are hardly effected by high pressure, but significant drop in CO_2 permeability was observed at elevated temperature. Simulations of CO_2/CH_4 separation by MCHF and polymeric membranes were conducted based on Aspen Hysys® integrated with ChemBrane, and the

process was optimized for cost calculation based on membrane area and compression energy. Simulation results indicated that the required separation can be achieved by a single stage process for MCHF, while a two-stage process is needed for the polymeric membranes.

Key words: Carbon membrane; Pore tailoring; Module construction; Thermal expansion; membrane simulations

1. Introduction

Methane is the main component of natural gas which also contains undesired components, such as CO_2, H_2O, N_2 and H_2S. The removal of these impurities is vital to meet the pipeline specification, and for this application the membranes fit well to selectively separate out CO_2 from the high-pressure gas mixture. This separation is the focus of this work. The demand for natural gas demand has increased by around 2.7% per year over the last decade with a total consumption of 3.47 trillion cubic meters in 2015, and this consumption drives a worldwide market of over $5 billion per year for new natural gas separation equipments. The market for gas separation membranes is expected to grow from US$ 150 million in 2002 to around US$ 750 million in 2020 [1-3].

The CO_2 needs to be separated to meet pipeline specifications (<2%) as it is corrosive, reduces the calorific value of natural gas and increases compression cost for transport of the gas [4]. Amine absorption is considered the most mature technique to separate out CO_2, but the limitation of regular maintenance and continuous operator care hinder the use of amine absorber-strippers at distant locations [5]. Membrane separation has advantages like the compact modular design, simple operation, small footprints, low capital and operational cost, environmentally friendliness and easy maintenance [3]. However, membrane processes have <5% of the natural gas sweetening market, as this technology is still facing challenges to overcome the plasticization and degradation of the membrane (caused by H_2O, CO_2, C_{4+} hydrocarbons and aromatic compounds). There is a further limitation of the membranes to process small/medium gas flows (<50,000Nm^3/h) [4, 6]. The natural gas stream is typically treated at their elevated pressure of 30-60 bar and may also contain impurities like mist of higher hydrocarbons and fine particles that can easily deposit on the membrane surface. Most of the commercially available membranes are polymeric and some of these membranes have shown high performance for CO_2/CH_4 separation, but high-pressure separations are still a challenge as these membranes are plasticized under high pressure or high CO_2 concentration

operations, and there are more chances of elevating market shares if other membrane materials are commercially produced [4-9].

Inorganic membranes with excellent thermal and chemical stabilities have been reported by many researchers. Particularly, carbon membranes have shown higher permeability and selectivities than commercially available polymeric membranes and have advantages in high pressure and temperature applications [8, 10-14]. Permeation through carbon membranes is accomplished by the adsorption of gas molecules and activated transport through selective pore openings.

The increase in performance (permeability and selectivity of a preferred gas) of the membrane cuts the capital cost, as less area is required to treat the same volume of gas. Numerous methods are being used to enhance the performance of carbon membranes and most of them involve changing precursor, precursor geometry, and pyrolysis conditions. Variations in these factors offer desirable carbon membrane morphology and tailored microstructure resulting in desired permeation properties [15-23]. A recent study has reported CO_2/CH_4 pure gas selectivity of 204 (CO_2 permeability of 83.1 Barrer) using PBI/Kapton as precursor [13]. Very limited data is available about the pore tailoring method after the pyrolysis. The CO_2 permeance of 0.021 (m^3(STP)/m^2.bar.h) and CO_2/CH_4 selectivity of 246, improved by pore tailoring technique of previously pyrolyzed hollow fibers has been reported [10].

The objective of this work is to explore the potential applicability of carbon hollow fibres (CHF) membranes at elevated pressure and temperature. Additionally, membrane pore tailoring was performed by using CVD and thermal treatment to obtain optimum selectivity and improved performance of previously pyrolyzed fibers. Despite high performance and mechanical stability of carbon hollow fiber membranes at high pressure and temperature, limited research has been done on this topic [24-27]. These authors [14] performed high pressure (70bar) experiments with a CO_2-CH_4 mixture, and they showed that carbon membranes offer selectivity and mechanical stability also at this pressure. Kruse et al. [28] have recently reported high pressure testing of carbon tubular membranes at 200 bar for a binary mixture of CO_2 with O_2, N_2 or He which showed promising results for high pressure and high temperature applications.

This research work addresses the comparison of the CHF performance with the performance of modified carbon hollow fibers (MCHF). The permeation properties of MCHF were enhanced by changing the pore geometry using oxidation, chemical vapor deposition (CVD) and reduction processes. Furthermore, module construction process for high pressure-temperature applications is reported in the current work. These modules were tested to separate

CO_2 at high pressure and elevated temperature. Finally, simulations were performed and discussed to estimate the economics of membrane process in natural gas separation application. The CHF were synthesized at a pilot scale plant using regenerated cellulose precursor, pyrolyzed in presence of N_2 at 550 $^{\circ}$C, and the membrane modules were tested at a maximum pressure of 70bar and maximum a temperature of 120 $^{\circ}$C in order to study the effect on membrane performance and durability of both fibers and potting material. Further, some experiments were performed to understand the bore side feed configuration effect and the burst pressure for the carbon hollow fibers. Burst pressure value for the MCHF was calculated as 700 bar using Barlow`s equation (based on the measured tensile strength of the MCHF).

2. Experimental

2.1 *Materials*

Acros Organics (Belgium) supplied cellulose acetate (CA: M_w 100,000) and 1-Methyl-2-pyrrolidone (NMP: Mw 99.13). Polyvinylpyrrolidone (PVP: M_w 10,000) was purchased from Sigma Aldrich (Norway). Ionic exchanged water was used for coagulation. Epoxy for module construction was received from Loctite (Norway). Steel piping was obtained from Brødrene Dahl, Norway. Steel housing and flanges were specially designed by MemfoACT AS. Gas cylinders for permeation testing were purchased from Yara Praxair: 99.96% purity for single gases (Norway).

2.2 *Preparation of carbon hollow fibers*

The carbon hollow fiber membrane which was investigated is a semi-commercial membrane, produced by MemfoACT AS (Norway), a company which has now closed down. The average pore size of the membrane is about 4 Å. The precursor is CA which is mixed with NMP and PVP to make dope solution. CA hollow fibers were synthesized using the dry-wet spinning process at a commercial scale plant, delivered by Philos, Korea. The prepared hollow fibers were then treated with NaOH for deacetylation. Then a tubular furnace (Carbolite®) was used to carbonize the deacetylated fibers. Procedure details for the production can be found in the patent by Hagg and Lie [29]. The protocol was optimized with respect to mechanical properties of the carbon membranes and its separation properties.

2.3 *Construction of high-pressure CHF module*

This chapter provides details on module construction, choice of epoxy, repair of broken fibers inside a module, and finally gas separation testing which is the ultimate quality control.

2.3.1 *Potting/Sealing*

Membrane modules were constructed using up to 3000 carbon hollow fibers with outer diameter between 0.15 and 0.25mm. The length of the finished module was 800mm. Manually sorted fibers were bundled loosely with wool thread so that fibers are held together while inserting in the stainless-steel tube as shown in fig. 1(a). The outer diameter of the SS-pipe was 32mm with 1.5mm of wall thickness. Edges of the tube were trimmed to smoothen the surface so that the small ending parts/end plug (named smart plugs here, see figure 1(b and e)) can be glued on. Then the fiber bundle was carefully pulled through the tube and a thread was tied onto the section of the bundle facing up. Then a piece of duct tape was placed on the bottom side as shown in fig. 1(b). The module side with dead end fibers (1b) was first exposed to extra fast curing adhesive (Loctite 9455) for fiber ends clogging, so that the sealing glue (Loctite 9483) was not sucked into the fibers. The fibers in the module was adjusted to be freely suspended inside the module (not touching the duct tape in the bottom facing smart plug). The module was fixed vertically in a clamp and glued by filling adhesive in the right amount to achieve a hermetic sealing. A period of 24 hrs was required for the glue to fully cure at room temperature. However, three hours were sufficient to turn the module upside down and glued the other end. A plastic cup with the same diameter as the steel tube was used to prepare a glue plug with a significant length of fibers suspended within the plug. Loctite 9483 was filled through the holes in the smart plug until glue reached the gas holes. Figure 1(d) presents the specially designed smart plug used on “open endings” side of the fibers and a glue plug with fiber endings (white dots) is shown on the top.

When sealing is cured after 24 hours at room temperature, hack saw, chisel together with rubber hammer was used to open the fiber endings on the top side of the module. After opening all fibers, modules were tested for any leakage.

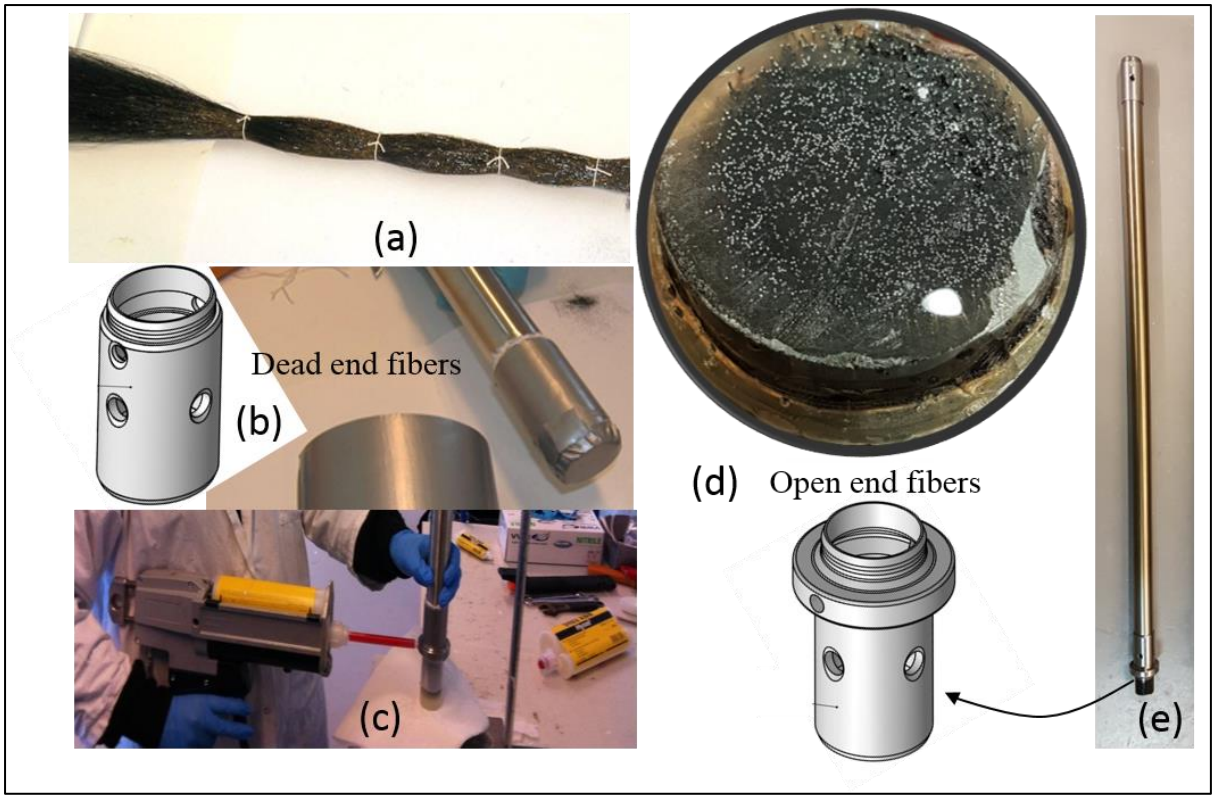

Figure 1: CHF module construction process, (a) CHF loosely bundled with thread, (b) smart plug and dead end potting, (c) filling glue on top end of the fibers (d) Open end fibers and smart plug (e) Module ready for testing broken or damaged fibers

2.3.2 *Selective clogging*

CHF were quality controlled after carbonization regarding straightness, length and broken fibres by hand sorting and throwing away all broken, too short, collapsed and fused fibres. However, it is not attainable, at least currently to prevent some broken or damaged fibres to remain in the fibre bundle when the membrane package in figure 1(a) is produced. This leads to a bundle consisting of three principal fibre types (good fibres, broken fibres, and surface damaged fibres) randomly distributed. It has been investigated, the possibility of using what is known as selective clogging of faulty fibres. The idea of this process is reported elsewhere [30], however, the procedure was developed at MemfoACT. The outline of this process is indicated in figure 2.

The membrane package is partly mounted into a pressure vessel in such a manner that the fibre end is exposed to the surroundings. By applying vacuum to the outer surface of the fibre, the lift flow force in the failed fibre types can easily be estimated using the Hagen Poiseuille equation (equation 1) if surface effects are ignored. However, the inner fibre diameter is only 0.19 mm (190 µm) so the capillary forces can most likely not be ignored, and the capillary rise

(or lowering) is estimated via the Pascal equation (equation 2), which requires knowledge about both surface tension of glue on carbon (our carbon consists of randomly oriented graphene sheets).

$$\frac{dx}{dt} = \Delta P \frac{r^2}{8\eta x}\phi, \quad x = \sqrt{\Delta P \frac{r^2 \cdot t}{8\eta}} \tag{1}$$

Where x is the penetration height, ΔP is the pressure difference (~1 bar), r is the internal radius of the fibre (95 µm), t is the time the pressure works (approximated as the pot life of the glue) and η is the viscosity of the liquid mixed glue.

$$x = \frac{2g \cdot \cos\theta}{r \cdot \rho \cdot \gamma} \tag{2}$$

Where γ is the surface tension of glue on carbon, θ is contact angle between glue and carbon, ρ is density of glue, g is the acceleration of gravity.

As shown in fig. 2, fibres marked as blue are good fibres, yellow are broken fibres, green colour represents the surface damaged fibres, and grey colour is showing clogged fibres after selective clogging process. Loctite 9492 and 9484 was used for selective clogging. As shown in fig. 2(b), the membrane module was clamped in upside down position. The glue was mixed in a pot and kept under the module in such a way that the fibre endings from the glue plug of the module are dipped in it. Now apply the vacuum for 1-2 minutes so that the required penetration is achieved and let it cure. Then cut the glue plug up to 3-5cm in length depending upon the glue type. The glue types used here have the penetration rise in this range for the good fibres. Now all the broken fibres are clogged because these fibres have maximum penetration rise. It is difficult to estimate the exact penetration rise for the surface damaged fibres. In practice, only 30-40% surface damaged fibres were clogged by selective clogging process. Therefore, manual clogging was done to identify and block the remaining damaged fibres. For the manual clogging, the module was clamped facing open fibres endings in upward direction. Slight over pressure than atmospheric pressure was applied instead of vacuum. Then soap or thin layer of

liquid water was poured on the glue plug to identify the fibres with fastest flow (making the bubbles faster). Using magnifying glass, the fibres with fastest gas flow were marked with a coloured marker. Now wipe the liquid and apply the vacuum again before using some instant glue (Loctite 3040 here) on marked fibres. In case of manual clogging (dark grey fibres), more than one fibre (including good fibres) is blocked while clogging the one defected fibre as fibres are packed closely together. Therefore, this process reduces the membrane effective area as well.

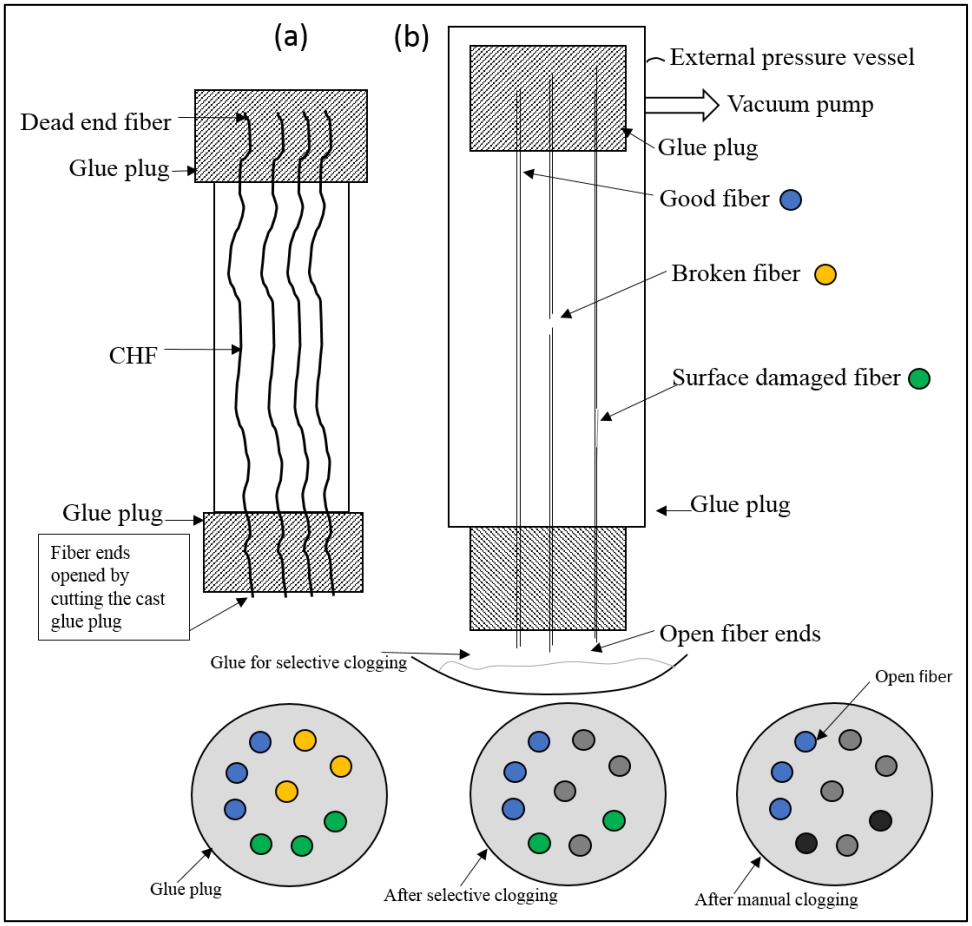

Figure 2:(a) Membrane Package, (b) Selective clogging of failed fibers in membrane package

Several glue types were tested for selective clogging application by studying both self-penetration of glue and forced penetration (under vacuum). Some of the glues are shown in

table 1. It was determined that the requirements for a suitable glue that could be used for selective clogging are as follows in prioritized order:

1. The glue must have an overall forced penetration height of about 10 cm,
2. The capillary rise alone must not be more than 1 cm.
3. The glue should cure into a solid plug inside the fibres (not form a gel, or plastic/ rubber)
4. Preferably cure within an hour (at least enough to be removed from the vacuum)
5. For analytical purposes, it is an advantage that the glue has a colour other than clear or black.

Table 1: Types of glue tested for selective clogging

Glue type [Loctite]	[b]Viscosity [Pa.s]	[b] Pot life [s]	Estimated viscous height (eq. 1) [mm]	Measured penetration total [mm]	[a] Measured capillary rise [mm]
3430	23	600	77	45	0
9466	35	3600	152	50	0
9455	5	420	138	90	3
9483	7	3600	341	>140	18
3421	95	9000	146	>100	4
9484	110	2400	70	50	0
9464	97	2000	68	20	0
9492	50	900	63	30	0

[a]The zero values can indicate capillary lowering due to a non-wetting glue (θ>90°), [b]Provided by suppliers

2.3.3 *Permeation testing*

For the permeation experiments discussed here, CHF modules were tested in a pilot scale temperature and pressure rise permeation system with shell side feed configuration. The system was constructed to tolerate high pressure single gas tests (CO_2, N_2, O_2). The mass transport properties of CHF were measured with the single pure gases CO_2 and N_2 at different feed pressure and experiments were carried out with no sweep on the permeate side. He et al. [31] has performed the mixed gas experiments on carbon membrane (prepared with alike protocol) and results showed that the membrane performance for CO_2 separation is the same or even higher in some cases for mixed gas as compared to single gas separation. Due to fire hazard limitations, CH_4 was not tested at the membrane production facility, only in a dedicated field. Therefore, the values for CH_4 gas are estimated values (selectivity $\alpha\ CO_2/CH_4 = 3 \cdot \alpha\ CO_2/N_2$), as shown in table 2.

Table 2: Membrane permeances and selectivities used in this work

Membrane Type	Permeance, (m^3(STP)/(m^2.h.bar)) [GPU[c]]		Selectivity	Wall thickness (μm)	Ref.
	CO_2	CH_4	CO_2/CH_4		
CHF[a]	4.14E-07 [1.51E-04]	6.89E-08 [2.52E-05]	6	41	This work
MCHF[b]	2.12E-02 [7.748]	8.53E-05 [3.12E-02]	249	41	This work
Polyimide	5.60E-02 [20.46]	1.70E-03 [6.21E-01]	33	125	[32]
CA	1.40E-01 [50.12]	9.10E-03 [3.326]	15	130	[3, 33]

[a]carbon hollow fibers without pore tailoring/modification, [b]carbon hollow fibers after pore tailoring process
1 [c]GPU = 2.736E-03 (m^3(STP)/(m^2.h.bar))

The performance of the membrane was evaluated by measuring the CO_2 permeance in [m^3(STP)/ (m^2·h·bar)] and CO_2/N_2 selectivities (α) using equations (3) and (4). A high-pressure vessel used for permeation tests is shown in figure 3. The tests were run from several hours to several days, to ensure that the transient phase of diffusion was passed and steady state obtained (dp/dt tends to a constant). The gas permeance, P [m^3(STP)/ (m^2·h·bar)] was evaluated using the equation 3.

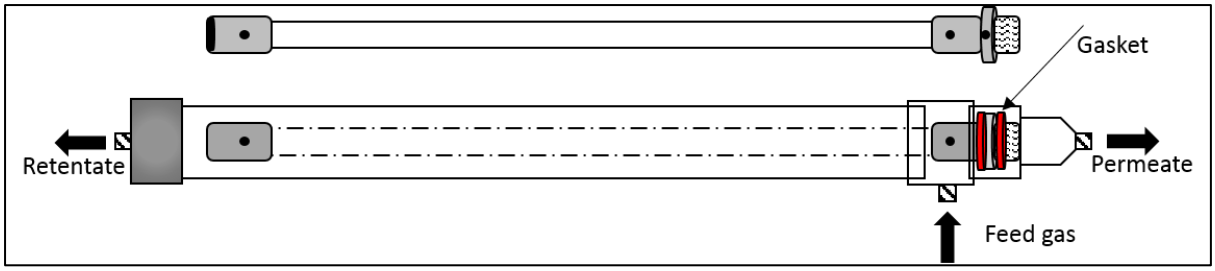

Figure 3: Membrane module in high pressure vessel for permeation testing

$$P = \frac{9.824.V \cdot (dp/dt)}{\Delta P \cdot A \cdot T_{exp}} \quad (3)$$

Here, V is the permeate side volume (cm^3) that can be measured with a pre-calibrated permeation cell reported elsewhere [34, 35]. However, the permeate side volume for this study was estimated by the tube length and cylinder volume on the permeate side. dp/dt and A are

the collection volume pressure increase rate (mbar/s) and total active area of membrane (cm^2) respectively, ΔP (bar) the pressure head and T_{exp} (K) is the temperature for experiment. The ideal selectivity was defined as the ratio of the pure gas permeances as shown in equation 4.

$$\propto_{A/B} = \frac{P_A}{P_B} \quad (4)$$

2.4 *Pore size adjustment*

The CHF modules after permeation tests were modified to enhance the membrane performance. For this purpose, modules were installed in a custom designed rig to allow the potting material (temperature limitations) to remain outside the heated area, with integrated external cooling of the potting during the process. The Fig. 4 illustrates the steps followed in this work, as also explained in the patent held by Soffer et al. [30].

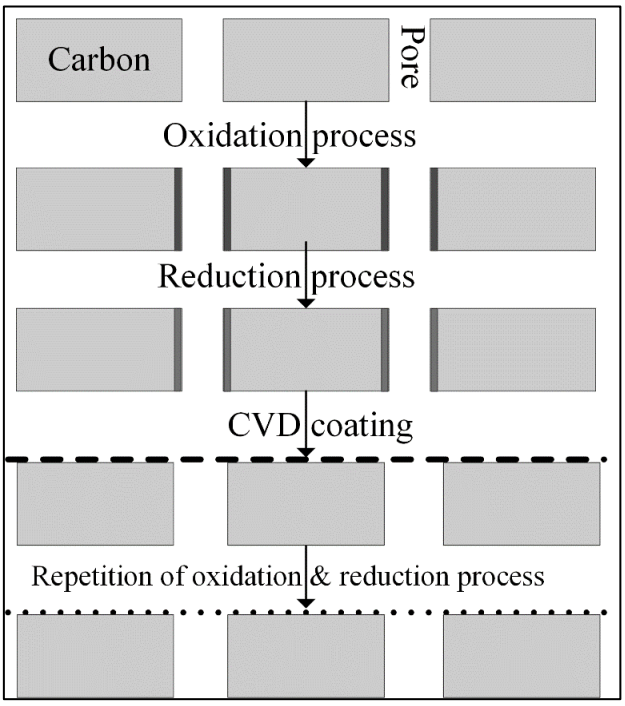

Figure 4: Steps followed for pore tailoring of CHF

The virgin carbon will most likely have too narrow pores to yield a feasible permeability, and the whole membrane wall thickness is expected to contribute to mass transfer resistance. Thus, the overall permeance of the carbon is infeasible low for practical usage. Due to the narrow pores, the selectivity is expected to be high (i.e. the selectivity of CO_2 over methane is normally

more than 100). A mild oxidation in synthetic air at about 300 °C for a defined time will cause the pores to widen. The internal pore surface of the carbon is now obviously in a highly-activated condition and will most likely exhibit a rapid clogging if exposed to water or any other hydrogen bonding molecules. (The carbon in this condition is surface wise like a process aged carbon. Hence, this and the following steps might also be modified to be a regeneration technique for the degenerated modules. The process is normally referred to as thermal regeneration)

The surface is deactivated using hydrogen at ca 500 °C, which will widen the pores slightly more. The permeance of the carbon is now significantly increased (normally, several orders of magnitude higher) and the selectivity is now expected to approach unity.

Chemical vapor deposition (CVD) using propene for a short time will cause a new layer of carbon to be generated on all accessible surfaces. The thickness of this layer is a strong function of reaction time and hence a thin layer of new virgin carbon with calculable thickness is achieved. This will lead to a decrease in flux and an increase in selectivity. Subsequent post oxidation and reduction may be needed to achieve the desired transport properties for the membrane module.

In this study, the post oxidation has been scrutinized, applying the concept of full factorial experimental design to investigate the influence of air pressure, air flow and reaction time. The design consisted of two levels and two replicas for the three parameters, in total 16 tests. Reaction time was 15-90 min, pressure difference over membrane was 1bar against vacuum and 1.4bar against vacuum, and airflow 1.5-12 l/h as shown in table 3.

Table 3: Parameters used for Post Oxidation-reduction and CVD process

Gas type	Heating rate [a] /Temperature	Pressure [b] (bar)	Gas flow [b] (l/hr)	Duration (min)
Heating 1				
Synthetic air [a]	4 °C/min	1.4 bar	<1	[b]
Postoxidation 1				
O_2 (20%) [a]	300 °C	1.4 bar	<1	[b]
Heating 2				
N_2 [a]	4 °C/min	1.5 bar	<1	[b]
Postreduction 1				
H_2 [a]	500 °C	1.4 bar	<1	30 [a]
CVD				
Propene [a]	500 °C	1.1 bar	1.5-12	[b]
Cooling 1				
N_2 [a]		1.2 bar	<1	[b]
Postoxidation 2				
O_2 (20%) [a]	300 °C	1 bar	<1	[b]
Heating 3				
N_2 [a]	4 °C/min		<1	[b]
Postreduction 2				
H_2 [a]	500 °C		<1	30 [a]

[a] *Fixed parameter,* [b] *varying parameter*

2.4.1 *Procedure for pore tailoring process*

Figure 5 presents the set-up used for post oxidation-reduction and CVD process. The module was connected within the furnace, in a way that the sealing glue is kept outside the oven as shown in figure 5. Glue cannot withstand temperature above 150 °C, therefore it was kept cold by chilled water. An insulation between furnace and heat exchanger was also applied. Then module and lines connected to the module were evacuated using vacuum pump down to 50mbar. To start first post-oxidation, the gas (synthetic air) bottle was opened and pressure/flow values were adjusted per protocol (e.g. 1bar and 10ml/min). The oven was programmed for the protocol (e.g. 4 °C/min to 300 °C, dwell 180min, cooling) and turned on. When the temperature in the cooling sequence is below 100 °C, the vacuum pump was switched off and the gas supply was stopped. Now 2nd heating sequence was started using N_2 atmosphere using same protocol until it reached 500 °C, then switched the gas to H_2 for first post-reduction process and kept for 30 min. After post-reduction, CVD was started using propene gas and then the cooling process was initiated swapping again to N_2 until the temperature goes down to 300 °C for the 2nd post-oxidation process as shown in table 3. The module can be removed from the oven when the temperature is below 40 °C.

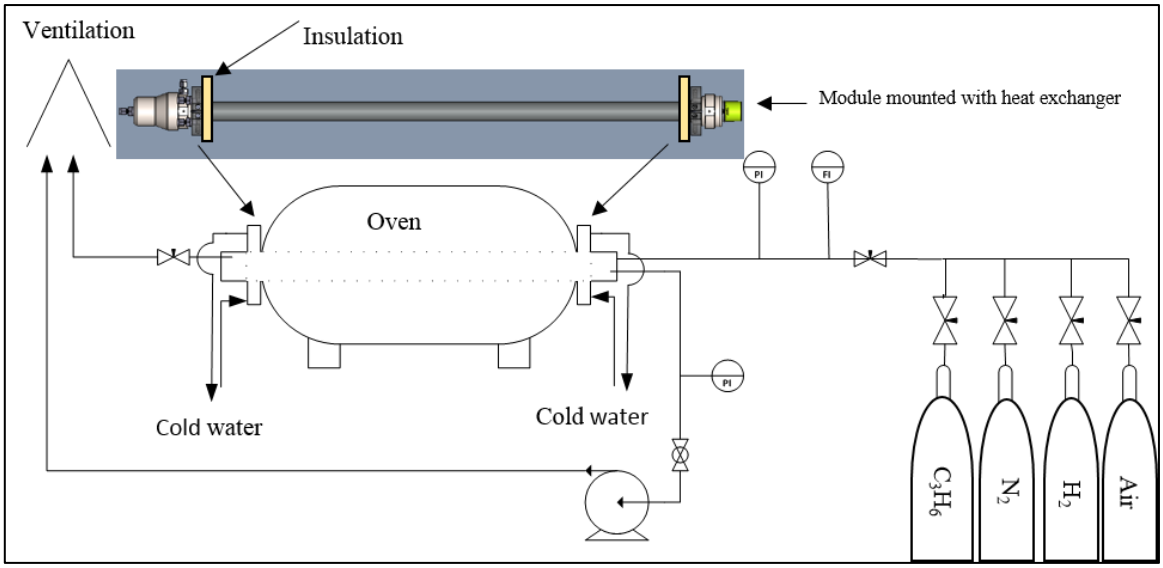

Figure 5: Post oxidation and CVD process

3. Simulation basis and process conditions

The following basis and assumptions were used to simulate the membrane process performance:

- Countercurrent gas transportation without sweep on permeate side has been used in all hollow fibre membrane modules.
- Membrane simulation model (Chembrane) was integrated into 9V Aspen Hysys®. This model, developed at NTNU, uses fourth-order Runge-Kutta method to calculate the flux along membrane length, and then iteration over permeate values to converge to a solution.
- CO_2 (0 - 50 %) is considered in the gas stream entering the membrane system. Process conditions used in simulations are shown in table 4. Due to the limitation caused by plasticization, CA membranes are simulated for maximum 30% CO_2 contents in feed at 50 bar, whereas maximum 50% CO_2 is considered for other membranes [36]. Permeabilities and selectivities used in simulations are shown in table 2.

Table 4: Process conditions used in simulations

Feed composition	0-50 % CO_2, balance CH_4
Feed flow rate (Nm^3/hr)	300
CH_4 purity in product (%)	98
CH_4 loss (%)	2.5
Feed pressure (bar)	50
Temperature (°C)	25
Flow pattern in membrane module	Countercurrent

- The adiabatic efficiency of the compressors is modelled as 75%.
- A single stage process can obtain methane recovery over 97.5% with MCHF, so this membrane is simulated for single stage, and other membranes are simulated for two stages. Simulating a two-stage system, permeate from the first stage is compressed to 51 bar and taken as the input for second stage membrane. Then rejection/retentate stream at 50bar from the second stage is recycled back to mix with feed stream which is already at 50bar. A two stage system is shown in figure 6.
- In a two-stage system CO_2 obtained on "permeate 2" is 97.5% pure and can be used further for re-injection in enhanced oil recovery process or some other application. In order to reduce the compression capacity/duty for CO_2, the pressure for permeate 2 is kept at 4bar in these simulations (as membrane area is assumed to be cheaper than an extra stage of the compressor at low pressure).

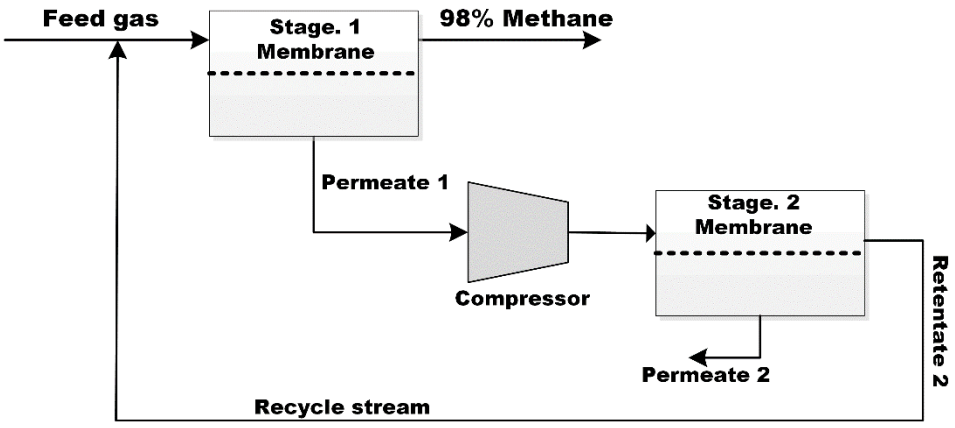

Figure 6: Two stage membrane process

4. Results and discussion

Thermal expansion is a critical parameter and to understand the stability of CHF in applications where they are exposed to varying temperature conditions, it is important to study the thermal expansion behavior of the CHF. Thermal stability of CHF in responding to change in temperature from 43-400 °C was studied.

4.1 *Thermal expansion of the CHF*

CHF were placed into a thermos thread hole in an alumina thermocouple tube and cut into the right length so that 10mm of the fiber was visible over thermocouple tube. Close clamping of the fibers was avoided so that thermal expansion difference would not introduce mechanical distortion. Thermocouple tube stood into a 3mm hole in a steel slab. The sample was placed in an optical dilatometer (MIZURA HTM, Expert Systems) and heated at a rate of 2 ˚C/min in the air till it reached the set point of 400 °C. The sample was filmed during the entire heating and cooling cycle. The sample was held at 400 ˚C for 5 minutes. Figure 7 is the snapshots from heating cycle. It indicates that the fibers are intact and stable up to 374 ˚C. Above this temperature, the change is probably because of oxidation.

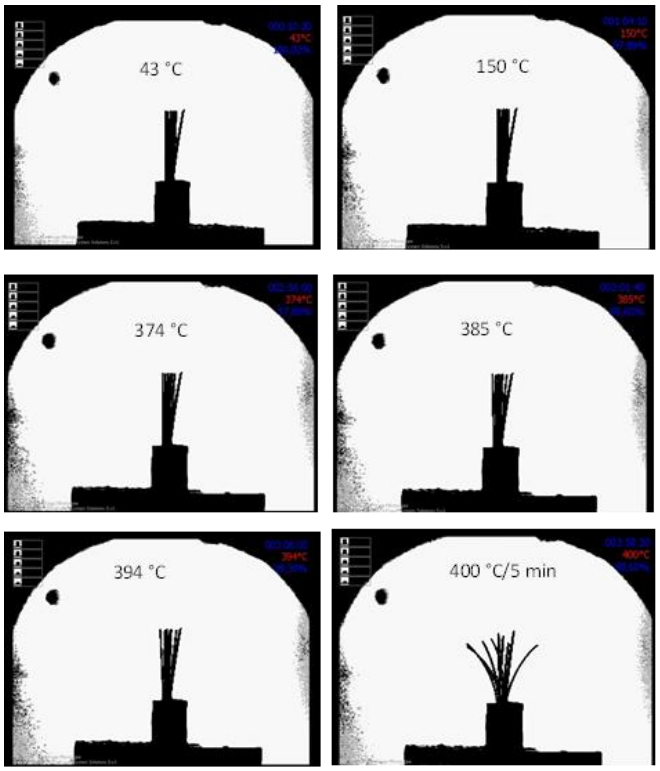

Figure 7: Snapshots of the thermal expansion of CHF

4.2 *CHF and MCHF (Performance difference)*

A total of 70 CHF modules of effective area range 0.2-2m^2 for each module (pore size might be in range 3-5Å as it was not detected by TEM and BET), were modified to study the effect of pore tailoring process and separation performance of CHF and MCHF. The result is shown in fig. 8. Single gas N_2 and CO_2 permeation tests were performed (using standard pressure-rise set up [37]) before and after modification at 23 °C, 5bar feed (shell-side configuration) pressure and vacuum on permeate side. Permeation results measured by pressure increase method indicated that overall performance of all modules was improved after physicochemical treatment of the membrane surface, and performance for most of the MCHF is high above the Robeson's upper bound 2008 as shown in figure 8 [38]. Maximum permeance value for a MCHF module was recorded (module 16), which was 50,000 times higher than prior to modification. CO_2/CH_4 selectivity was improved 41 times in comparison with pre-modified fibers of the same module. This selectivity and permeance value is used in the simulation section. In a few modules, selectivity was reduced after surface treatment and the reason may be that the chemical vapor deposition process did not create a sufficient layer on all the fibers, or that the oxidation-reduction process opened the pores too void before or after the CVD process. Numerical values of CO_2/CH_4 selectivity, CO_2 permeabilities, membrane area for CHF and MCHF are shown in table A.1 of Appendix A. The modules referred in fig.8 all contain between 200 -2000 fibers.

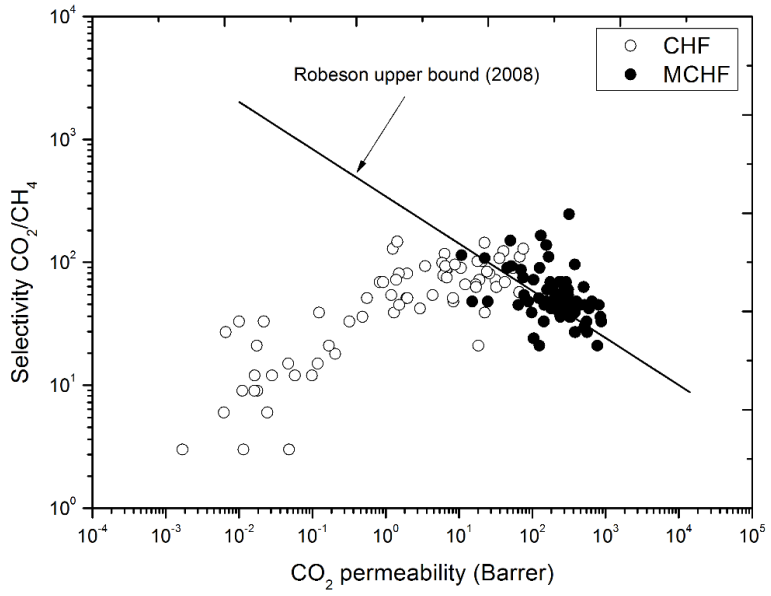

Figure 8: Separation performance of CHF and MCHF (1 Barrer = 2.736.10E-09 m^3(STP).m/m^2.bar.h)

4.3 *High pressure testing*

The permeation properties of MCHF were also examined at elevated temperature and pressure. A membrane module consisting of two modified hollow fibers was used for high pressure experiments to understand the behavior of pure gas CO_2 and N_2 permeation (fluxes) at seven different pressure set points for shell-feed configuration as shown in figure 9. All experiments were done at 1 bar pressure on the permeate side. Both CO_2 and N_2 flux remained almost constant with increase in pressure. Rao et al. [39] explained that with very strong adsorbing or non-permanent gases pore blocking can occur at high pressure resulting in high selectivity. Permeabilities of N_2 and CO_2 changes, but the effect is much smaller and it explains that the dominant mechanism here is molecular sieving, which is not being effected by pressure. It was found that the carbon membrane is not swollen by high partial pressures of CO_2. Fibers were fed to shell side, however, pressures higher than 70bar were not tested at our facility due to HSE (health and safety executive) limitations. Although in the later stage, dynamic mechanical properties of MCHF were measured and then burst pressure was calculated by using Barlow`s formula (equation 5). Then fibers were kept bore side fed at 60bar (10% CO_2 in N_2) for 1 hour. It was observed that fibers are quite stable when fed through bore side as well.

$$P = \frac{2S \cdot T}{(OD)} \tag{5}$$

Here, P (psi) is the fluid pressure, S (psi) is allowable stress (ultimate tensile strength or yield strength can be used), T(in) wall thickness of the fiber, OD(in) is outside diameter of the fiber.

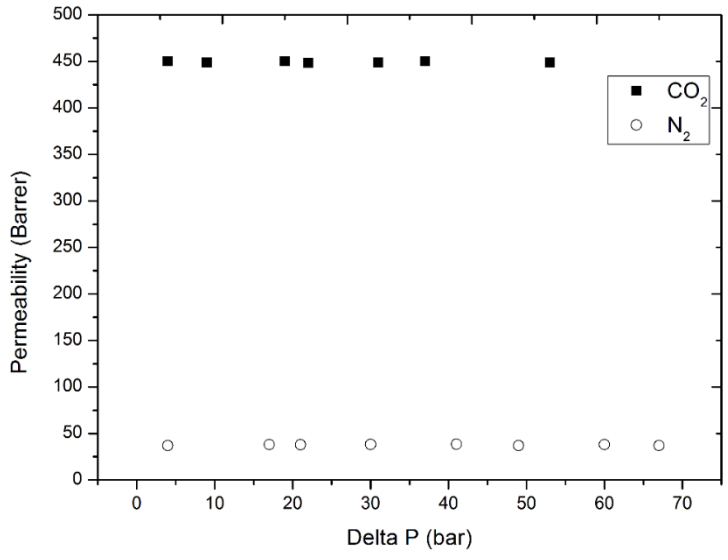

Figure 9: CO_2 and N_2 permeability at elevated pressure (T:23 °C)

4.4 *Elevated temperature testing*

To investigate the temperature dependence of mass transport through the MCHF, pure gas CO_2 and N_2 has been studied between 23 and 120 °C as shown in figure 10. The extensive temperature span shows that CO_2 and N_2 have different transport behavior with the temperature elevation. For inert gases, the separation can be done at temperatures up to the carbonization temperature (~500-800 ˚C). If the operational temperature is limited by the sealing material, this may be overcome by installing heat exchangers at the module ends. As shown in fig. 10, CO_2 permeability declines significantly almost 50% in a linear fashion when the temperature is increasing. Fuertes et al. [40] suggested that the CO_2 permeability decline at high temperature and low pressure is a result of a compensation between increasing mobility and decreasing adsorption. In contrast, the effect of temperature on N_2 permeability was very low and above 45 °C, the permeability of N_2 is almost constant.

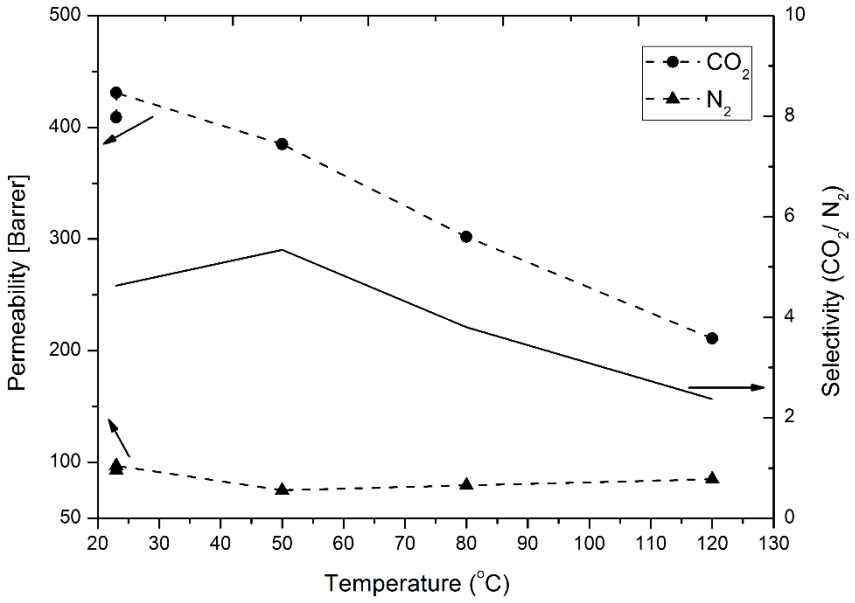

Figure 10: Effect of temperature on the permeability of CO_2 and N_2 (P: 5bar)

4.5 *Simulations and economics*

In this study, the effect of CO_2 contents in feed for a fixed product purity (98% CH_4) and loss (2.5% CH_4) using membranes with different efficiencies is simulated and hence the subsequent effect on total cost in form of membrane area and compression duty is evaluated. Selection of a separation process is entirely based on economic considerations. Costs must be calculated for

every specific separation problem in details and it cannot be considered very general. This article gives a short capital cost comparison among MCHF, polyimide and CA membranes, which include the capital cost of the membrane and installed compressor for required duty as shown in equation 6. No recompression/pumping cost for the CO_2 produced is considered here. Detailed economic design and net present value (NPV) calculations for CO_2-CH_4 separation with MCHF membranes are explained in the referred article [10]. Carbon membranes are quite advanced membranes and still in the optimization process. That is why the cost per m^2 mounted into a module for MCHF is four times higher than CA as shown in table 5. This price for MCHF membranes is for carbon membranes prepared from CA (assumed as economical raw material) on a pilot scale plant (MemfoACT, Norway). This price is estimated from the pilot-scale production experience. However, the prices for polymers are taken from the data presented by W. J. Koros [41] at NTNU, Norway. These values were further used by other authors also [11, 31]. Membrane properties used in simulations are shown in table 2.

$$C_{total} = C_{membrane} + C_{compressor} \qquad (6)$$

Table 5: Economic parameters

Membrane type	CA	Polyimide	MCHF
Cost \$/m^2	25	50	100
Compressor cost (\$)	\$ 8700 x (HP^a)$^{0.82}$		

[a] *HP is the installed horse power for the installed compressor*

The membrane performance (CO_2 permeability and selectivity) influences the CO_2 removal rate from the feed gas. The higher performance will reduce the membrane area needed for separation to achieve the product purity. In the case of polyimide, the selectivity is higher than CA, but the permeance is much lower which results in overall slightly lower performance as compared to CA. In simulations, pressure for permeate one (fig. 6) is kept at 1 bar for both CA and polyimide membranes. In the case of polyimide membrane, the optimized pressure can achieve the selectivity-driven region by increasing area on the first stage and reducing compression energy on 2nd stage (considering membrane area is cheaper than compression energy). Figure 11 shows that area required for both polyimide and CA is almost same for different CO_2 concentrations in the feed gas. Due to low selectivity, it is not possible to achieve required product purity in a single stage while using CA or polyimide membrane system. Therefore, a two-stage system is needed for required CH_4 purity and recovery and in that case,

and compression is needed on 2nd stage to achieve the pipeline pressure for recycle stream as shown in fig. 6. This compression duty is shown in figure 11 which is alike for both CA and polyimide membranes.

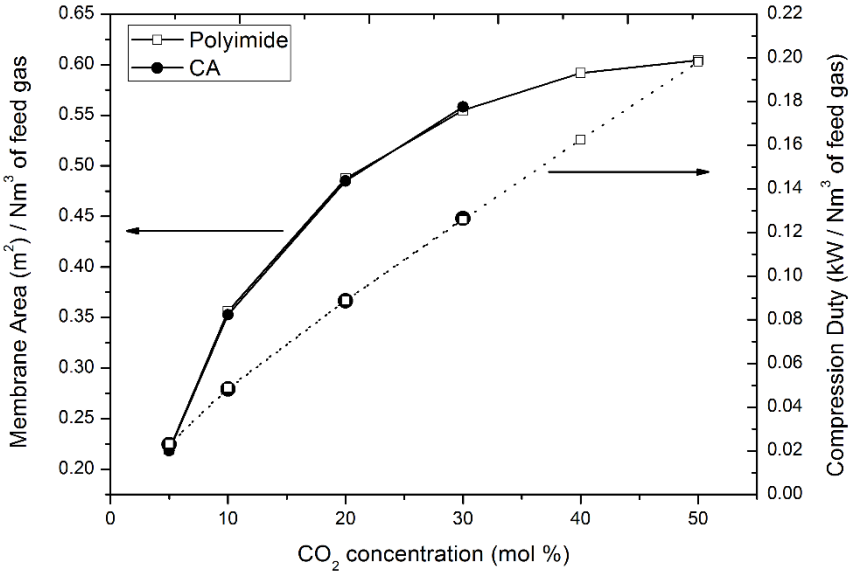

Figure 11: Effect of CO_2 contents in feed on Area and duty for two-stage membrane system

The modified carbon membranes offer high efficiency in a one stage process reducing methane losses, footprint, and energy consumption as shown in fig. 12. Results indicate that CH_4 recovery of 99.2% can be achieved in a single stage with MCHF membrane system when 5% CO_2 is present in the feed gas. Required area is almost constant from 20% and higher contents of CO_2 in natural gas. The data in fig. 6 depends on pressure ratio, which is fixed here at 50/1 bar.

For the natural gas facility, in the case of single stage separation, the largest cost item is the membrane and associated housing for high pressure, because there is not any compression cost associated with natural gas feed, which is already at high pressure. But in the case of two stage membrane system, the need for compression of recycle stream adds up the cost as shown in figure 13. From the results, for the natural gas stream, increasing the membrane performance (both permeability and selectivity) reduces the process complexity by achieving the goal in a single stage and hence reduces the total cost. Although MCHF membrane price is higher than polyimide and CA membranes, still the separation process with MCHF is economical and offers small foot prints owing to only single stage requirement. Carbon hollow fiber membranes are still in the development phase, and the membrane price will most likely be

reduced by further optimization of the carbon membrane production and modification process in the future.

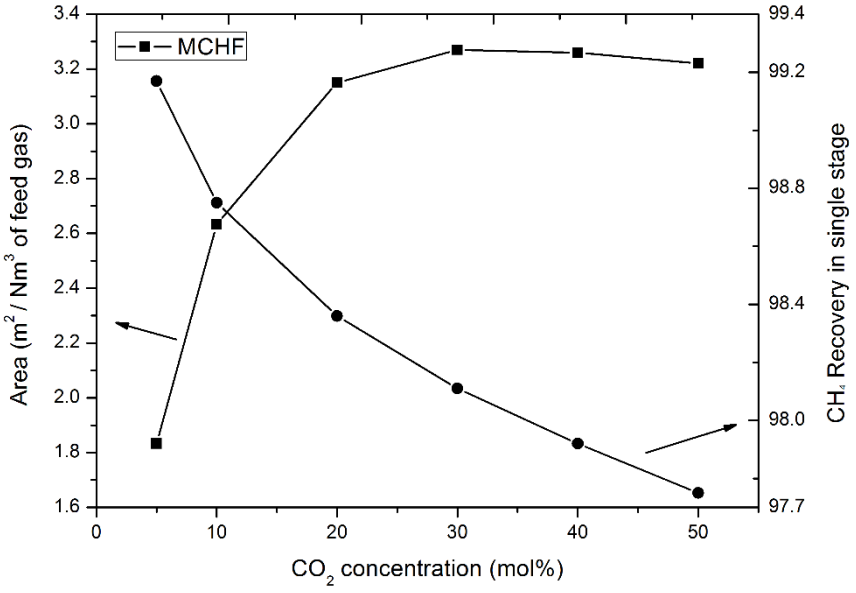

Figure 12: Required membrane area and CH_4 recovery in a single stage MCHF system

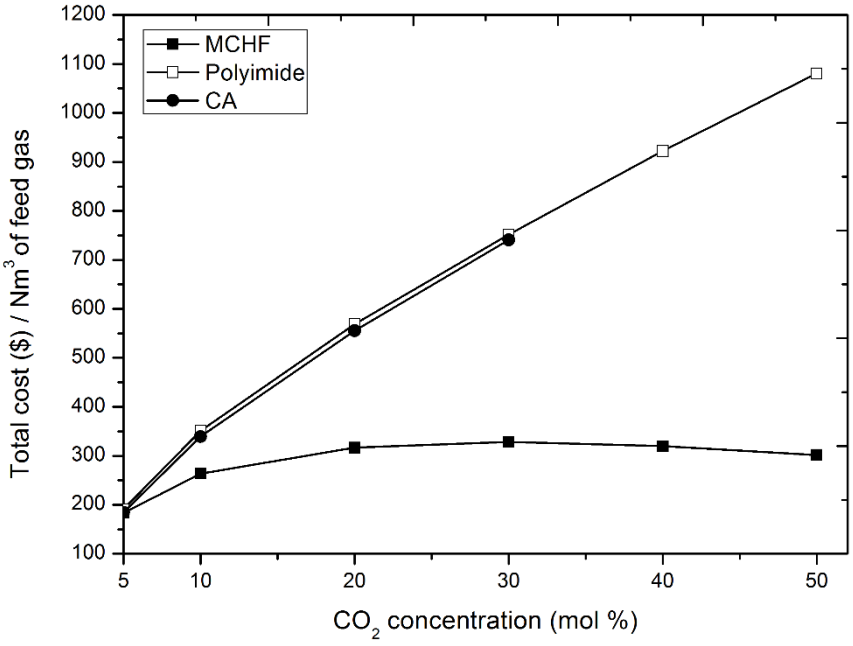

Figure 13: Total cost per Nm^3 of feed for CA and polyimide two-stage membrane process and MCHF single stage process

4.6 *Carbon membrane applications*

Membranes have been widely used in natural gas treating to pipeline specification and enhanced oil recovery (EOR), where CO_2 is removed from an associated natural gas stream and reinjected into the oil field to improve oil recovery. Carbon membranes have the ability to separate gases based on small differences in the size and shape of the gas molecules and separation performance is higher than conventional polymeric membranes. High CO_2 concentration and low flow favour carbon hollow fibres membrane processes. Stand-alone membrane systems are ideal for small distributed fields with small gas flows (<20 million scfd / < 23,600 Nm^3/h). Membrane area is dictated by the percentage of acid gas removal rather than absolute acid gas removal, and small variations in feed acid gas content hardly change the sales-gas purity. In the case of MCHF, the membrane has high performance which keeps the membrane far into the selectivity driven region and the installed area is not much effected by CO_2 contents in the feed. Simulation data showed that installing a MCHF membrane area for 20% CO_2 contents can work for CO_2 range of 1-50% with less than 1% loss in both purity and recovery. Installing membrane area for equal or below 5% CO_2 contents brings it into the pressure ratio driven region and additional compression cost adds up, (pipeline purity and recovery) if actual CO_2 concentration increases in the line. A schematic plot (adopted from Baker and Lokhandwala [5]) illustrating the effect of gas flow rate and CO_2 composition on the choice of the separation process is shown in figure 14.

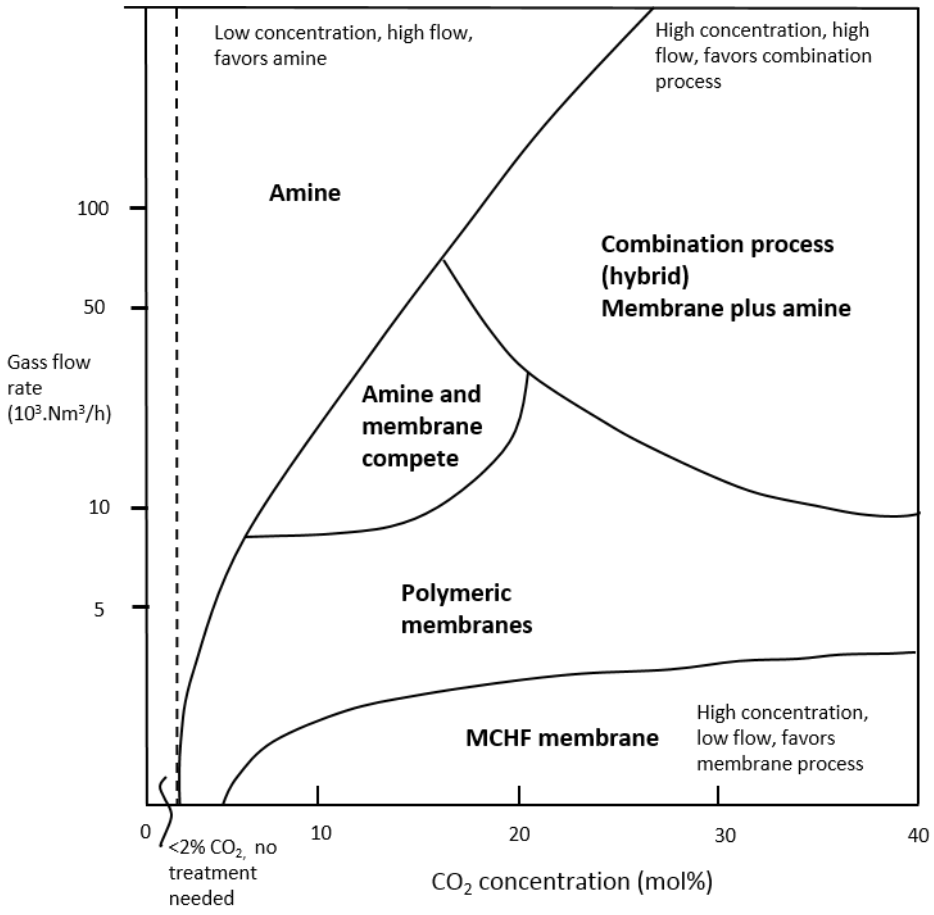

Figure 14: MCHF application region in "gas flow rate and CO_2 concentration diagram" adopted from Baker and Lokhandwala [5]

5. Conclusion

Cellulose acetate hollow fibers were spun and deacetylated with NaOH at a pilot scale facility. These hollow fibers were carbonized in N_2 environment up to 550 °C based on a multi-dwell carbonization protocol. Numerous potting glue types were tested to make stable modules of CHF for high pressure and elevated temperature permeation testing. A potting/sealing procedure with selective clogging and thermal expansion of CHF were presented. Permeation properties of CHF were investigated for the single gases CO_2 and N_2 at the pilot facility. Due to fire hazard limitations, CH_4 was not tested at membrane production facility, only in the lab. CHF modules were further modified to enhance the permeation properties by tailoring pore structure with an oxidation-reduction process and forming a new thin selective layer of carbon using CVD with propene. The MCHF showed attractive permeation properties for CO_2, N_2, and CH_4 at elevated temperature and pressure conditions. It appeared that permeation properties for CO_2/CH_4 remained almost constant by increasing pressure up to 70 bar, but

significant decline (almost 50%) in CO_2 permeability was observed when the temperature was increased up to 120 °C. Using permeation results for MCHF simulations were conducted based on Aspen Hysys® integrated with ChemBrane. The CO_2/CH_4 separation process was optimized based on membrane area and compression duty to calculate the cost for the given CH_4 purity and recovery. A cost comparison for MCHF, polyimide, and CA membranes was presented, which showed that MCHF can do CO_2/CH_4 separation in a single stage, making the process economical and simple as compared to polymeric membranes where a complex two stage system is required to do the same separation. Offering high permeability and high CO_2/CH_4 selectivity, MCHF is far into the selectivity driven region and simulation data showed that a MCHF system designed for 20% CO_2 contents in feed can separate the range of 1-50% CO_2 contents in the feed with less than 1% loss in purity and recovery. The successful high-pressure (up to 70 bar) testing of MCHF is encouraging and industrially relevant for many high-pressure applications, such as CO_2 removal from natural gas.

Acknowledgement

The authors would like to thank The Department of Chemical Engineering at NTNU for providing the possibility to work with this article.

References

[1] British Petroleum, British Petroleum Statistical Review of World Energy. 65th Edition, (2016). https://www.bp.com/content/dam/bp/pdf/energy-economics/statistical-review-2016/bp-statistical-review-of-world-energy-2016-full-report.pdf (accessed 12.02.2017).

[2] *U.S. Energy Information Administration* EIA-0383, Annual Energy Outlook with projections to 2040 (2015). https://www.eia.gov/outlooks/aeo/pdf/0383(2015).pdf (accessed 15.01.2017).

[3] R. W. Baker, Future Directions of Membrane Gas Separation Technology. *Ind Eng Chem Res* **41** (2002), 1393-1411. http://pubs.acs.org/doi/abs/10.1021/ie0108088.

[4] R. W. Baker, Membrane Technology and Applications. 2nd ed. John Wiley & Sons Ltd. California , 2004, pp 338.

[5] R. W. Baker, K. Lokhandwala, Natural gas processing with membranes: An overview. *Ind Eng Chem Res* 47 (2008), 2109-2121. http://pubs.acs.org/doi/abs/10.1021/ie071083w6.

[6] M. Mulder, Basic Priciples of Membrane Technology. 2nd Ed. Kluwer Academic Pulishers, Netherlands, 1996.

[7] X. He, T.-J. Kim, M.-B. Hägg, Hybrid fixed-site-carrier membranes for CO2 removal from high pressure natural gas: Membrane optimization and process condition investigation. *J. Membr. Sci.* 470 (2014), 266-274. http://dx.doi.org/10.1016/j.memsci.2014.07.016.

[8] W. N. W. Salleh, A. F. Ismail, Carbon membranes for gas separation processes: Recent progress and future perspective. *J. Membr. Sci. Res.* 1 (2015), 2-15, http://www.msrjournal.com/article_12301.html

[9] T.-J. Kim, H. Vrålstad, M. Sandru, M.-B. Hägg, Separation performance of PVAm composite membrane for CO2 capture at various pH levels. *J. Membr. Sci.* 428 (2013), 218-224, http://dx.doi.org/10.1016/j.memsci.2012.10.009.

[10] Y. Kusuki, H. Shimazaki, N. Tanihara, S. Nakanishi, T. Yoshinaga, Gas permeation properties and characterization of asymmetric carbon membranes prepared by pyrolyzing asymmetric polyimide hollow fiber membrane. *J. Membr. Sci.* 134 (1997), 245-253, http://dx.doi.org/10.1016/S0376-7388(97)00118-X.

[11] S. Haider, A. Lindbråthen, M.-B. Hägg, Techno-economical evaluation of membrane based biogas upgrading system; a comparison between polymeric membrane and carbon membrane technology. *Gr. En. & Env.* 1 (2016), 222-234. http://dx.doi.org/10.1016/j.gee.2016.10.003.

[12] M. Yoshimune, K. Haraya, CO2/CH4 Mixed Gas Separation Using Carbon Hollow Fiber Membranes. *En. Proc.* 37 (2013), 1109-1116, http://dx.doi.org/10.1016/j.egypro.2013.05.208.

[13] S. S. Hosseini *et al.*, Enhancing the properties and gas separation performance of PBI–polyimides blend carbon molecular sieve membranes via optimization of the pyrolysis process. *Sep. Pur. Tech.* 122 (2014), 278-289. http://dx.doi.org/10.1016/j.seppur.2013.11.021.

[14] D. Q. Vu, W. J. Koros, S. J. Miller, High Pressure CO2/CH4 Separation Using Carbon Molecular Sieve Hollow Fiber Membranes. *Ind. Eng. Chem. Res.* 41 (2002), 367-380, http://pubs.acs.org/doi/abs/10.1021/ie010119w.

[15] K. Briceño, D. Montané, R. Garcia-Valls, A. Iulianelli, A. Basile, Fabrication variables affecting the structure and properties of supported carbon molecular sieve membranes

for hydrogen separation. *J. Membr. Sci.* 415–416 (2012), 288-297. http://dx.doi.org/10.1016/j.memsci.2012.05.015.

[16] H.-H. Tseng, K. Shih, P.-T. Shiu, M.-Y. Wey, Influence of support structure on the permeation behavior of polyetherimide-derived carbon molecular sieve composite membrane. *J. Membr. Sci.* 405–406 (2012), 250-260. http://dx.doi.org/10.1016/j.memsci.2012.03.014.

[17] W. N. W. Salleh, A. F. Ismail, Effect of Stabilization Condition on PEI/PVP-Based Carbon Hollow Fiber Membranes Properties. *Sep. Sci. Tech.* 48 (2013), 1030-1039. doi: 10.1080/01496395.2012.727938.

[18] A. C. Lua, Y. Shen, Preparation and characterization of polyimide–silica composite membranes and their derived carbon–silica composite membranes for gas separation. *Chem. Eng. J.* 220 (2013), 441-451. http://dx.doi.org/10.1016/j.cej.2012.11.140.

[19] Teixeira M, Campo M, Tanaka DA, Tanco MA, Magen C, Mendes A. Carbon–Al2O3–Ag composite molecular sieve membranes for gas separation. Chem. Eng. Res. and Desig, 90(2012):2338-45. doi: http://dx.doi.org/10.1016/j.cherd.2012.05.016.

[20] C. W. Jones, W. J. Koros, Carbon molecular sieve gas separation membranes-I. Preparation and characterization based on polyimide precursors. *Carbon* 32 (1994), 1419-1425, http://dx.doi.org/10.1016/0008-6223(94)90135-X.

[21] A. B. Fuertes, T. A. Centeno, Carbon molecular sieve membranes from polyetherimide. *Micropo. and Mesopo. Mat.* 26 (1998), 23-26, http://dx.doi.org/10.1016/S1387-1811(98)00204-2.

[22] J. E. Koresh, A. Soffer, Mechanism of permeation through molecular-sieve carbon membrane. Part 1.-The effect of adsorption and the dependence on pressure. *Journal of the Chemical Society, Faraday Transactions 1: Phy. Chem. in Cond. Phases* 82 (1986), 2057-2063, doi: 10.1039/F19868202057.

[23] R. Steiner, Microfiltration and Ultrafiltration - Principles and Applications. L. J. ZEMAN, A. L. ZYDNEY Marcel Dekker, New York, 1996, 648 Seiten, Zahlr. Abb. u. tab., geb., $ 185,-, ISBN 0-8247-9735-3. *Chemie Ingenieur Technik* 69 (1997), 1479-1479 doi: 10.1002/cite.330691022.

[24] R. Swaidan, X. Ma, E. Litwiller, I. Pinnau, High pressure pure- and mixed-gas separation of CO2/CH4 by thermally-rearranged and carbon molecular sieve membranes derived from a polyimide of intrinsic microporosity. *J. Membr. Sci.* 447 (2013), 387-394, http://dx.doi.org/10.1016/j.memsci.2013.07.057.

[25] E. P. Favvas, Carbon dioxide permeation study through carbon hollow fiber membranes at pressures up to 55 bar. *Sep. Pur. Tech.* 134 (2014), 158-162, http://dx.doi.org/10.1016/j.seppur.2014.07.041

[26] G. Härtel, T. Püschel, Permselectivity of a PA6 membrane for the separation of a compressed CO2/H2 gas mixture at elevated pressures. *J. Membr. Sci.* 162 (1999), 1-8, http://dx.doi.org/10.1016/S0376-7388(99)00066-6.

[27] W. Ogieglo, L. Upadhyaya, M. Wessling, A. Nijmeijer, N. E. Benes, Effects of time, temperature, and pressure in the vicinity of the glass transition of a swollen polymer. *J. Membr. Sci.* 464 (2014), 80-85, http://dx.doi.org/10.1016/j.memsci.2014.04.013.

[28] N. Kruse *et al.*, Carbon membrane gas separation of binary CO2 mixtures at high pressure. *Sep. Pur. Tech.* 164 (2016), 132-137, http://dx.doi.org/10.1016/j.seppur.2016.03.035.

[29] M.-B. Hägg. J. A. Lie. Carbon Membranes, patent US patent 20100162887 A1, 2010. https://www.google.ch/patents/US20100162887

[30] A. A. Soffer, J. Gilron, H.Cohen, Separation of Linear from Branched hydrocarbons using a Carbon Membrane. US parent 5914434 A,1999. http://www.google.no/patents/US5914434

[31] X. He, J. A. Lie, E. Sheridan, M.-B. Hägg, Preparation and Characterization of Hollow Fiber Carbon Membranes from Cellulose Acetate Precursors. *Ind. Eng. Chem. Res.* 50 (2011), 2080-2087, doi: 10.1021/ie101978q.

[32] G. Dong, H. Li, V. Chen, Factors affect defect-free Matrimid® hollow fiber gas separation performance in natural gas purification. *J. Membr. Sci.* 353 (2010), 17-27, http://dx.doi.org/10.1016/j.memsci.2010.02.012.

[33] C. Liu, R. Bai, Preparation of chitosan/cellulose acetate blend hollow fibers for adsorptive performance. *J. Membr. Sci.* 267 (2005), 68-77, http://dx.doi.org/10.1016/j.memsci.2005.06.001.

[34] W.-H. Lin, R. H. and Chung, T.-S., Gas transport properties of 6FDA-durene/1,4-phenylenediamine (pPDA) copolyimides. *J. Polym. Sci. B Polym. Phys.* 38 (2000), 2703-2713, doi: 10.1002/1099-0488(20001101)38:21<2703::AID-POLB10>3.0.CO;2-B.

[35] J. A. Lie, Synthesis, performance and regeneration of carbon membranes for biogas upgrading – a future energy carrier. Norwegian University of Science and Technology, PhD thesis, 2005.

[36] G. Valenti, A. Arcidiacono, J. A. Nieto Ruiz, Assessment of membrane plants for biogas upgrading to biomethane at zero methane emission. *Biom. Bioenerg.* 85 (2016), 35-47, http://dx.doi.org/10.1016/j.biombioe.2015.11.020.

[37] K. C. O'Brien, W. J. Koros, T. A. Barbari, E. S. Sanders, A new technique for the measurement of multicomponent gas transport through polymeric films. *J. Membr. Sci.* **29** (1986), 229-238, http://dx.doi.org/10.1016/S0376-7388(00)81262-4.

[38] L. M. Robeson, The upper bound revisited. *J. Membr. Sci.* 320 (2008), 390-400, http://dx.doi.org/10.1016/j.memsci.2008.04.030.

[39] M. B. Rao, S. Sircar, Nanoporous carbon membrane for gas separation. *Gas Sep. & Pur.* **7** (1993), 279-284, http://dx.doi.org/10.1016/0950-4214(93)80030-Z.

[40] A. B. Fuertes, T. A. Centeno, Preparation of supported asymmetric carbon molecular sieve membranes. *J. Membr. Sci.* 144 (1998), 105-111, http://dx.doi.org/10.1016/S0376-7388(98)00037-4.

[41] W. J. Koros, Membrane opportunities and challenges for large capacity gas andvapour feeds, *European Membrane Society's 20th Summer School*, (2003), NTNU, Trondheim, Norway.

Appendix A

Table A.1: Carbon hollow fibers and Modified carbon hollow fibers performance

		CHF		MCHF	
No.	Area	Selectivity	CO_2 Permeability	Selectivity	CO_2 Permeability
	(m^2)	CO_2/CH_4	Barrer	CO_2/CH_4	Barrer
1	1.0	21	1.75E-02	60	1.60E+02
2	0.8	33	2.18E-02	48	2.46E+01
3	0.7	12	2.81E-02	24	1.05E+02
4	0.8	12	1.63E-02	39	9.82E+01
5	1.0	18	2.05E-01	45	6.47E+01
6	0.9	9	1.11E-02	69	1.76E+02
7	1.0	3	4.80E-02	72	1.04E+02
8	0.7	6	2.43E-02	54	3.10E+02
9	1.0	15	4.68E-02	138	1.55E+02
10	0.8	27	6.59E-03	60	3.08E+02
11	1.1	9	1.78E-02	45	1.78E+02
12	0.7	3	1.15E-02	69	2.52E+02
13	0.8	9	1.61E-02	51	1.23E+02
14	1.0	3	1.69E-03	57	2.62E+02
15	1.0	12	5.76E-02	42	5.96E+02
16	0.9	6	6.20E-03	246	3.18E+02
17	1.1	51	5.57E-01	48	3.39E+02
18	1.0	12	9.88E-02	165	1.31E+02
19	1.3	15	1.18E-01	21	1.25E+02
20	1.1	21	1.68E-01	42	2.93E+02
21	1.1	51	1.92E+00	45	2.45E+02
22	1.0	51	1.97E+00	42	1.80E+02
23	1.5	72	3.14E+01	36	2.42E+02
24	1.4	90	7.09E+00	39	2.90E+02
25	1.5	39	1.24E-01	48	8.76E+01
26	1.4	33	3.19E-01	39	2.35E+02
27	1.5	54	1.19E+00	48	2.40E+02
28	1.4	72	1.90E+01	42	2.52E+02
29	1.4	81	2.59E+01	39	3.80E+02
30	1.6	48	8.39E+00	36	3.23E+02
31	1.7	69	8.27E-01	36	3.34E+02
32	1.7	36	4.83E-01	57	2.80E+02
33	1.9	66	1.69E+01	45	2.94E+02
34	1.6	84	2.41E+01	27	3.87E+02
35	1.1	39	1.30E+00	45	3.06E+02

		CHF	MCHF		
No.	Area	Selectivity	CO_2 Permeability	Selectivity	CO_2 Permeability
	(m^2)	CO_2/CH_4	Barrer	CO_2/CH_4	Barrer
38	1.7	54	4.37E+00	60	1.89E+02
39	1.6	63	1.70E+01	48	2.77E+02
40	1.7	66	1.22E+01	21	7.71E+02
41	1.4	90	5.45E+01	30	5.16E+02
42	1.5	69	4.22E+01	27	5.60E+02
43	1.4	129	1.25E+00	45	1.46E+02
44	0.3	117	6.36E+00	33	1.44E+02
45	0.3	123	4.04E+01	36	8.55E+02
46	0.3	111	6.76E+01	33	8.76E+02
47	0.2	78	6.09E+00	33	5.51E+02
48	0.2	144	2.23E+01	48	4.02E+02
49	0.2	39	2.25E+01	45	5.20E+02
50	0.2	42	2.94E+00	96	3.82E+02
51	0.2	69	9.22E-01	69	2.88E+02
52	0.2	102	2.08E+01	48	1.53E+02
53	0.2	51	8.30E+00	93	5.16E+01
54	0.3	99	5.89E+00	108	2.25E+01
55	0.3	93	3.46E+00	150	5.03E+01
56	0.3	108	3.56E+01	45	4.54E+02
57	0.3	129	7.56E+01	48	6.55E+02
58	0.2	90	1.06E+01	69	2.32E+02
59	0.3	102	1.79E+01	45	8.05E+02
60	0.2	75	6.82E+00	63	5.04E+02
61	0.2	81	1.96E+00	111	1.68E+02
62	0.2	81	1.52E+00	66	1.85E+02
63	0.3	93	6.49E+00	51	2.03E+02
64	0.1	147	1.44E+00	114	1.08E+01
65	0.3	72	1.39E+00	90	1.26E+02
66	0.3	96	8.83E+00	48	2.99E+02
67	0.9	45	1.53E+00	90	4.57E+01
68	1.0	21	1.84E+01	75	7.52E+01
69	0.9	57	6.65E+01	87	7.02E+01
70	1.1	33	1.00E-02	48	1.51E+01